Journal of Physico-Chemical Material (JPCM)
Volume 1, Issue 1, Date: 31-December-2024
ISSN: 2978-4468, DOI: 10.64820/AEPJPCM.11.7.12.122024

First Principles Study on the Structural and Electrochemical Properties of $LiCoO_2$ and Ni Doped $LiCoO_2$ Cathodes in Lithium Batteries

Rodney N. Abugre [1], G. K. Nkrumah-Buandoh [2], S. A. Atarah [3] and G. G. Hagoss[4]
[1, 2, 3, 4] Department of Physics, University of Ghana, Accra, Ghana
Email: [1]rabugre@ug.edu.gh /rabugre1@gmail.com
*Rodney N. Abugre

Abstract*—First principles computational approach on the Structural and Electrochemical properties of undoped $LiCoO_2$ and Ni doped $LiCoO_2$ is studied with Vesta Application Software and Density Functional Theory calculations on Quantum Espresso Package. Results from the study indicate doping $LiCoO_2$ with Ni increases the cell voltage and reduces the rate of formation of oxygen vacancies ensuring there is structural stability of the cathode during the lithium process of charging and discharging. Overall, the Structural and Electrochemical properties of Ni doped $LiCoO_2$ as cathode material is greatly improved increasing the life span as compared to the intrinsic $LiCoO_2$ as cathode material for battery applications.

Keywords*— Physico-chemical properties; structural properties; electrochemical properties; crystal structure properties; Density functional theory

I. INTRODUCTION

The increasing fuel cost and periodic shortages, along with the public awareness of 'greenhouse' effects, has made it highly desirable to develop Electric Vehicles (EV), instead of fossil fuel vehicles, with a low greenhouse gas emission. However, commercial applications of Electric Vehicles will not be realized if advanced energy storage systems with an efficient energy saving and emission reduction cannot be successfully developed [1]. Lithium-Ion Batteries (LIB's) have received intensive research and development focus because of their high energy density, long cycle life, and superior environmental friendliness [2]. For Electric Vehicle storage battery applications, the performance of Lithium-Ion Batteries, with regards to their energy density, safety, and cost, need to be significantly improved. A lithium-ion battery is composed of three essential components namely the Li+ intercalation anode, cathode, and the electrolyte/separator. Li+ ions move from the cathode to the anode through the electrolyte/separator during charging and back when discharging, and simultaneously, the electrons flow out of the external circuit to provide the electrical power. Although the efficiency of energy conversion for LIBs depends on a variety of factors, their overall performance strongly relies on the structure and property of the materials used. The key to success in the development of advanced LIBs to meet the emerging EV market demands is the electrode materials, especially the cathode [3]. The cathode costs nearly twice as much as the anode. This could be attributed to the fact that the working voltage, energy density, and rate capability of Lithium-Ion Batteries are mainly determined by the limited theoretical capacity and thermodynamics of the cathode material in the present Lithium-Ion Battery technology. It is therefore critical to develop promising cathode materials for the current Lithium-Ion Battery technology [4]. To develop improved lithium-ion battery electrode materials that exhibit high energy density, high power, better safety, and longer cycle life. The acceleration of materials discovery, synthesis, and optimization will benefit from the combination of both experimental and computational methods[5, 6, 7 & 8]. First principles (ab Initio) computational methods have been widely used in materials studies/ science and can play an important role in accelerating the development and optimization of new energy storage materials. These methods can prescreen previously unknown compounds and can explain complex phenomena observed with these compounds [9 &10]. First principles (ab initio) modeling refers to the use of quantum mechanics to determine structure or property of materials. Ab initio computation methods are best known for precise control of structures at the atomic level constituting perhaps the most powerful tool to predict structures, and with computational quantum mechanics, many ground state properties can be accurately predicted prior to synthesis. More importantly, the reliability and accuracy of the computational approaches can be significantly improved if experimental information is well integrated to provide realistic models for computation. Experiments and computations are complementary in nature. Many intrinsic properties of electrode materials, including voltages, structure stability, lithium diffusivity, bandstructure, and electronic hopping barriers can now be computed accurately with first-principles computation methods [11&12]. In this research, first principles computational methods are used to study the structural and electrochemical properties of $LiCoO_2$ and Ni doped $LiCoO_2$ materials as cathodes in Lithium batteries.

Received: 24-6-2024
Revised: 25-7-2024
Published: 31-12-2024

This article is freely accessible under the Creative Commons Attribution License, allowing for its use, distribution, and reproduction in any format, as long as the original work is correctly cited. © 2024 The Authors.

II. THEORY

One of the most useful quantities that is calculated for each compound is its formation energy, the energy required to form positive formation energy or the energy given off by forming negative formation energy of a compound from its constituent elements. Compound formation energies are required to predict compound stability, generate phase diagrams, calculate reaction enthalpies and voltages including the determination of other material properties [13]. In general, the mathematical expression for the formation energy of a compound (∇H_f) is given by

$$\nabla H_f = E_{tot} - \sum_i \mu_i x_i \quad (1)$$

where E_{tot} is the DFT total energy of the compound, μ_i is the chemical potential of element i and x_i is the quantity of element i in the compound. The standard convention is to take the chemical potential of each species to be the DFT total energy of the elemental ground state. The computed formation energy of a compound is valid at 0 K.

A. Cell voltage

The volumetric or gravimetric energy density of a battery depends on the open circuit voltage (OCV). Thus, materials that provide a high voltage along with an electrolyte that is stable at this voltage are crucial for developing high energy density batteries. The voltage of a battery, V(x), depends on the chemical potential of the cathode and anode [14] and is defined as

$$V(x) = \frac{\mu_{cathode}(x) - \mu_{anode}(x)}{zF} (2)$$

Here, $\mu_{cathode}$ and μ_{anode} are the chemical potentials of the cathode and the anode, respectively, z is the number of charge units that are transferred, x is the chemical composition, and F is Faraday's constant. In the case of Lithium-Ion Batteries (LIBs) the value of z is typically 1. The chemical potential is related to the change in free energy with respect to the change in Li concentration in LIBs, the average equilibrium voltage can be written as

$$V = \frac{-\Delta G}{\Delta x F} (3)$$

Here, ΔG is the difference in free energy between the fully lithiated (discharged state) and delithiated states (charged state) and Δx is the number of Li ions transferred. For solid-state materials the entropic contribution to ΔG is expected to be negligible at room temperature [14, 15, 16 &17] and therefore the free energy difference, ΔG, can be approximated as the potential energy difference, ΔE. Therefore, equation 3 can be re-written as

$$V = \frac{-\Delta E}{\Delta x F} (4)$$

where the symbols have their usual meanings. ΔE can be approximated by the internal (potential) energy change per intercalated Li+ ion, since the vibrational and configurational entropy contributions to the cell voltage at room temperature are expected to be small. The change in total energy, E, of the system obtained from DFT calculations using equation 1 leads to a predicted cell voltage that is an average value for compositions between x_i and x_j (where $\Delta x = x_i - x_j$) in equation 4. In the case of the Li (de)intercalation reaction in $LiMO_2$, where M is an earth metal /transition earth metal element

$$Li_{x_i}MO_2 \rightleftarrows Li_{x_j}MO_2 + (x_i - x_j)Li (5)$$

The cell voltage, V can be written as

$$V = \frac{-E_{Li_{x_i}MO_2} - E_{Li_{x_j}MO_2} - (x_i - x_j)E_{Li}}{(x_i - x_j)F}, x_i > x_j (6)$$

The total energies of $Li_{x_i}MO_2$ ($E_{Li_{x_i}MO_2}$, $Li_{x_j}MO_2$ $\left(E_{Li_{x_j}MO_2}\right)$ and $Li(E_{Li})$ can be determined using electronic structure methods such as DFT. One can also compute the voltage as a continuous function of change in Li ion concentration, V(x), to generate a voltage profile. The voltage profile is more important for materials having multiple transition metals such as Nickel rich cathode materials (NCM), as the oxidation state of the transition metals varies with varying x. Moreover, the nature of the voltage curve can provide vital information about phase transitions occurring in the material as x changes [17, 18 & 19]. However, the voltage profile computation requires the structures of the materials at various values of x. Here, equation 6 can be used to obtain the average equilibrium voltage for different concentrations intervals, x and x + Δx.

For example, in the $LiCoO_2$ system this approach leads to Li (de)intercalation reaction in $LiCoO_2$ as $Li_{x_i}CoO_2 \rightleftarrows Li_{x_j}CoO_2 + (x_i - x_j)Li (7)$

where Co is a transition earth metal element and a cell voltage calculation of the form

$$V = \frac{-E_{Li_{x_i}CoO_2} - E_{Li_{x_j}CoO_2} - (x_i - x_j)E_{Li}}{(x_i - x_j)e}, (8)$$

where e is the electronic charge. In practice, if one lithium atom per formula unit is removed the voltage derived from the difference between the end members is equation 8.

B. Formation of Oxygen Vacancy

The formation energy of oxygen vacancy (E_f) refers to how much energy is required to remove an oxygen molecule from a compound and is defined as

$$E_f = E_{lim\,O_{2-x}} + \frac{x}{2}E_{o2} - E_{lim\,O_2} (9)$$

For the (de)lithiation reaction

$$lim\,O_2 \rightleftarrows LiMO_{2-x_i} + \frac{x_i}{2}O_2 (10)$$

where $E_{lim\,O_2}$, $E_{lim\,O_{2-x}}$ and E_{O_2} represent the total energies of $LiMO_2$, $LiMO_{2\text{-}x}$ and O_2 molecule respectively. The formation energy of oxygen vacancy determines how stable oxygen is in the lattice during the Lithium process of charging and discharging. A positive value of the formation energy of oxygen means oxygen in the lattice is stable hence oxygen vacancies are not easily formed. This implies oxygen cannot be easily released into the atmosphere preventing degradation of the cathode material in the battery. The larger the positive value the more stable oxygen is in the lattice and vice versa [17 ,19 & 20].

III. METHODS

Surface science data of $LiCoO_2$ having hexagonal closed packing crystal structure with lattice parameters $a = b =$

$2.8429 armstrong$, $c = 14.1456 armstrong$ and space group P3m1 is used to obtain the supercell structure of $LiCoO_2$ made up of 3 Lithium atoms, 3 Cobalt atoms and 6 Oxygen atoms. The supercell structure of $LiCoO_2$ is obtained with the use of the Xcryden Software Application. With the crystal structure and space group maintained, $LiCoO_2$ material is doped with Nickel by replacing one of the Cobalt atoms with Nickel leaving the rest of the Cobalt atoms in the now Ni doped $LiCoO_2$ material or creating a vacancy in the $LiCoO_2$ material by removal of one Cobalt atom and filling that vacancy with a Nickel atom. The supercell structure obtained for undoped $LiCoO_2$ and Ni doped $LiCoO_2$ is displayed on fig. 1. Vesta Software Application is used to construct the unit cell of $LiCoO_2$ and Ni doped $LiCoO_2$ using the information from the surface science data. Copper K alpha 1 (Cu Kα1) X-ray source with wavelength of 1.5409 Armstrong is used to determine the Reflection data along various miller indices (h k l) or plane directions by applying the Structural model on the Vesta Application software and the Power diffraction plot obtained by plotting a graph of intensity against two theta angles using the Reflection data obtained. The Power diffraction plot of undoped $LiCoO_2$ and Ni doped $LiCoO_2$ is displayed on fig. 2 and 3. The Isosurface plot is determined along the (1 1 1) plane direction of undoped $LiCoO_2$ and Ni doped $LiCoO_2$ unit cells with a resolution of 0.5 by the use of surface plot tool on the Vesta Software Application. Fig. 4 and 5 displays the Isosurface/ charge density plot of undoped $LiCoO_2$ and Ni doped $LiCoO_2$.

A. Structural Stability Method

Construct either a single unit cell or super cell of $LiCoO_2$ and Ni doped $LiCoO_2$ structure using the Vesta application software**.** The measuring tools on the Vesta Application software is used to measure the bond length between any two nearest neighboring atoms for three trials and the atomic radius for each atom used to calculate the bond length. Both measured and calculated bond length data is tabulated in table 1, with the shortest bond length ratio indicating the strongest bond strength (Covalent or Ionic bonds) or interaction between the two atoms involved.

B. DFT Computational Method

Electronic structure methods for obtaining the total ground state/ minimum energy is achieved using the First principles calculation with Spin Polarized Density Functional theory as implemented on the Quantum Espresso Software Package. Pseudopotential is Ultrasoft + core correction with augmented plane wave energy and charge density cut off of 25 Ry and 500 Ry respectively. The exchange correlation functional is described by Perdew-Burke-Ernzerhof (PBE) within the Generalized Gradient Approximation (GGA) with an electron beta mixing of 0.4. Convergence with respect to self-consistent iterations followed by non-self-consistent iterations is assumed when the total-energy difference between cycles is less than 10^{-6} eV/atom. For the geometric optimization of the crystal structure, the Brillouin zone (BZ) was sampled using the K-point sampling method of Monkhorst-Pack. Optimization of K-point grid densities over the BZ is achieved with Monkhorst- Pack by setting the electronic structure (super cell) to 5x5x1 for all First Principle Calculations for the total minimum energy, Fermi Energy level, Energy bandgap, density of state and more. The output from the Self Consistent Field iteration calculation for $LiCoO_2$ supercell, $Li_{x_j}CoO_2$ supercell with Li defect and $LiCoO_{2-x}$ supercell with oxygen molecule defect is used to determine the average voltage/ average intercalation potential and the formation energy of oxygen vacancy. Next, $LiCoO_2$ supercell structure is doped with Nickel to make the cathode Nickel rich and the above methods used to study the structural, electronic and electrochemical performance of $LiCoO_2$ employed in the study of Nickel doped $LiCoO_2$. Results from the study of $LiCoO_2$ and Ni doped $LiCoO_2$ is compared to determine the best material with suitable properties for use as cathodes in battery applications.

C. Results and Discussions

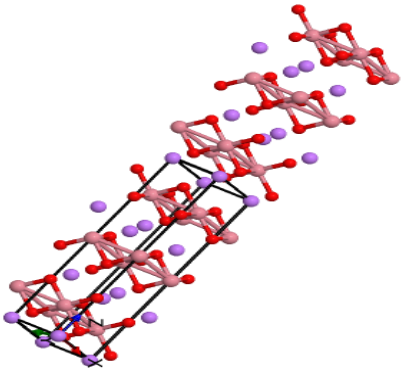

Fig. 1a.

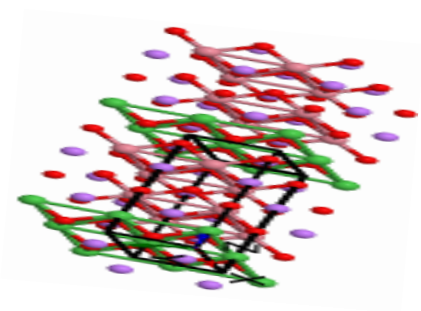

Fig. 1b.

Fig.1a and Fig. 1b: Displays the 2x2x2 supercell structure of $LiCoO_2$ & Ni doped $LiCoO_2$ respectively. The colour's red, pink, purple and green represent the Oxygen (O_2), Cobalt (Co), Lithium (Li) and Nickel (Ni) atoms respectively.

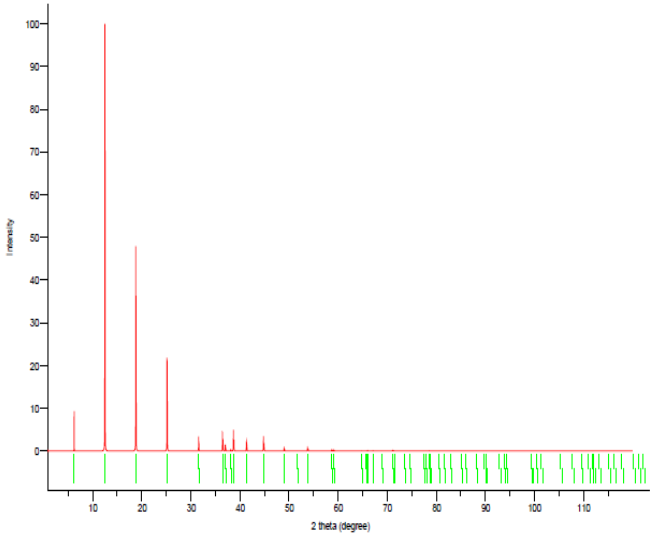

Fig. 2: Shows the Power Diffraction Pattern of Ni doped $LiCoO_2$.

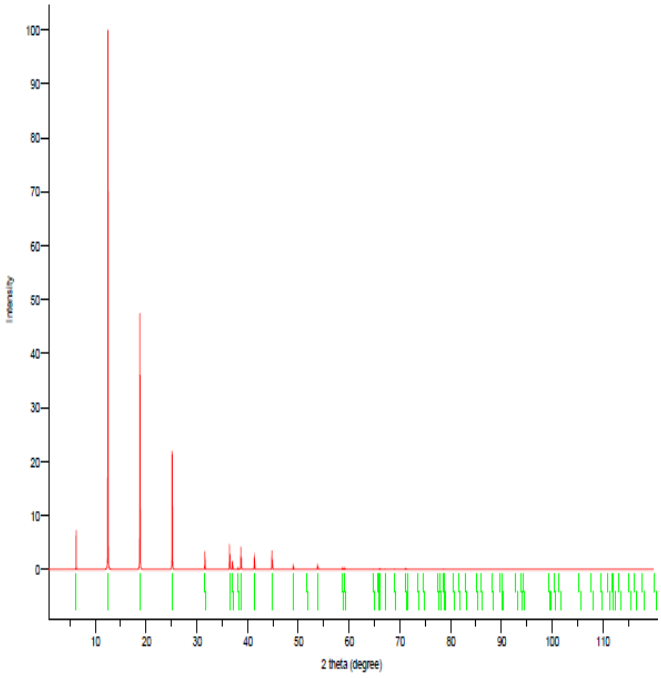

Fig. 3: Shows the Power Diffraction Pattern of undoped $LiCoO_2$.

Table 1:Bond length ratio between Li-O, Co-O and Ni-O

Atomic species	Atomic radius / Å	Calculated Bond length / Å	Measured Bond length/ Å	Ratio of Measured to Calculated
Li	1.57	2.31 Li-O	1.17516, 1.17516 1.17516, Li-O	0.758268
Co	1.25	1.99 Co-O	0.72842, 0.72842 0.72842, Co-O	0.366040
Ni	1.25	1.99 Ni-O	0.72842, 0.72842 0.72842 Ni-O	0.366040
O	0.74			

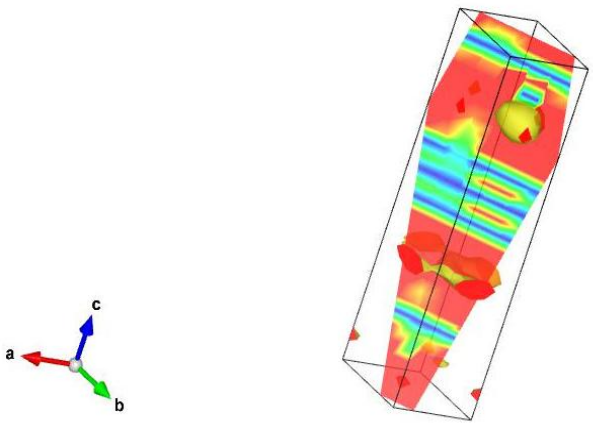

Fig 4: Displays the Isosurface/ charge density plot of $LiCoO_2$.

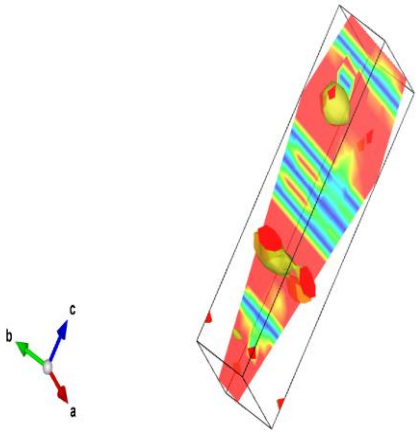

Fig 5: Isosurface or Charge density plot for Ni doped $LiCoO_2$.

The Power Diffraction plot displayed on fig. 2 and fig. 3 look similar as they both show four main peaks at approximately the same two theta angle values including some other phases. A careful look at the plot for both $LiCoO_2$ and Ni doped $LiCoO_2$ indicate that on Fig. 2, the four main peak intensities of 12.59594, 100.00, 59.50382 and 29.2897 lamina occur at two theta angles of 6.24315, 12.50494, 18.80448 and 25.16197 degrees respectively whilst on figure 3, the four main peak intensities of 5.3767, 100.00, 57.4889 & 28.3864 lamina occur at two theta angles of 6.24315, 12.5049, 18.8045 & 25.162 degrees respectively. Implying the peaks occur at the same two theta angles but with different peak intensities except for the highest peak intensity which remains same.This means there is a shift in the arrangement of atoms in the $LiCoO_2$ crystal structure due to the doping of $LiCoO_2$ with Ni accounting for the decrease in intensity values. Fig. 4 and fig. 5 displays the Isosurface / charge density plot along the (1 1 1) plane with 0.5 resolution. On the surface plot on both figures, Oxygen is the red portion, Lithium is the green section, Cobalt is the deep blue portion and Nickel is the black section lying in the middle of the deep blue portion (Cobalt) and red portion (Oxygen) as seen on fig. 5. The yellow

portions refer to accumulation of charges/electrons around atoms while the light blue portions refer to the withdrawal of charges/electrons by the surrounding atoms. On both figures, there is accumulation of charges between Oxygen & Lithium atoms (O-Li) and withdrawal of charges between Cobalt and lithium. However, on fig. 5 in addition to the withdrawal of charges between cobalt and lithium there is also withdrawal of charges between Nickel and Lithium atoms. This clearly indicates doping $LiCoO_2$ with Nickel causes some changes in the chemical reactivity of the $LiCoO_2$ system due to the additional accumulation and withdrawal of charges. Results on table 1 is used for comparing the bond length between Li-O, Co-O and Ni-O, with the smallest ratio implying strongest bond with oxygen thereby preventing the rapid release of oxygen from the cathode material during the Lithium process of discharging and charging. This means strong bonds between oxygen and the element in this case Cobalt or Nickel would reduce the rate of degradation and ensure there is chemical stability of the material to be used as cathodes with a long-life span. Hence during the lithium process Ni doped $LiCoO_2$ is predicted to be more stable than $LiCoO_2$ since Cobalt and Nickel both form strong bonds with oxygen.

Table 2: Displays the values of Fermi energy, Average intercalation potential and Energy of formation of oxygen.

compound	Fermi energy, eV	Cell Voltage V	Formation energy of Oxygen, eV
LiCoO2	12.14	3.08	-2.29
$LiCo_{1-y}Ni_yO_2$	11.44	35.56	62.55

From information on table 2, Ni doped $LiCoO_2$ has a lower fermi energy level than the intrinsic $LiCoO_2$. The cell voltage and the energy of formation of oxygen for Ni doped $LiCoO_2$ is higher than that for $LiCoO_2$. The inference is that the Electrochemical properties of $LiCoO_2$ cathode material is greatly improved when is doped with Nickel. The large value of formation energy of oxygen means oxygen in the Ni doped $LiCoO_2$ lattice structure is not easily released during the lithium process of charging and discharging as compared to the undoped $LiCoO_2$ cathode material. Hence oxygen in the Ni doped $LiCoO_2$ lattice structure is very stable, preventing degradation of Ni doped $LiCoO_2$ cathode material and increasing the life span of Ni doped $LiCoO_2$ cathode. However, the doping concentration ratio must be considered to obtain a desirable average voltage for battery applications.

D. Conclusion

Results from structural studies of $LiCoO_2$ and Ni doped $LiCoO_2$ indicate there is a shift in the arrangement of atoms in $LiCoO_2$ crystal structure due to the doping of $LiCoO_2$ with Ni which accounted for the decrease in intensity values as observed on the power diffraction plots. From the charge density plots, doping $LiCoO_2$ with Ni was found to cause some changes in the chemical reactivity of $LiCoO_2$ system due to the additional accumulation and withdrawal of charges. From the bond length ratios on table 1, Ni doped $LiCoO_2$ is predicted to be more stable than $LiCoO_2$ during the lithium process since Cobalt and Nickel both form strong bonds with oxygen. Comparing results tabulated on table 2, The average intercalation potential and the energy of formation of oxygen vacancy for Ni doped $LiCoO_2$ is higher than that for $LiCoO_2$ meaning the Electrochemical properties of $LiCoO_2$ cathode materials are greatly improved when doped with Nickel. Therefore, there is significant reduction in the rate at which oxygen is released during the lithium process and this decreases the rate of degradation of the Nickel rich $LiCoO_2$ cathode material thereby increasing the life span of Ni doped $LiCoO_2$ as cathodes in Lithium batteries.

ACKNOWLEDGMENT

Sponsor of this research work is the University Of Ghana, Africa – Ghana for the award of a PHD degree in Computational Physics.

REFERENCES

[1]. O. vanVliet, A.S.Brouwer, T.Kuramochi, M.vandenBroek, A. Faaij, "Energy Use, Cost and CO2 Emissions of Electric Cars," Journal of Power Sources 196 (2011) 2298–2310.

[2]. J.B. Goodenough, Y. Kim, "Challenges for Rechargeable Li Batteries" Chemistry of Materials 22 (2010) 587- 603.

[3]. J.M. Tarascon, M.Armand, "Issues and challenges facing rechargeable lithium batteries" Nature 414 (2001) 359–367.

[4]. D. Kovacheva, B. Markovsky, G. Salitra, Y. Talyosef, M. Gorova, E. Levi, M. Riboch, H.-J. Kim, D. Aurbach, Electrochimica, "Electrochemical behavior of electrodes comprising micro- and nano-sized particles of LiNi 0.5Mn 1.5O 4: A comparative study" Acta 50 (2005)5553–5560.

[5] Cathode materials for next generation lithium ion batteries Jiantie Xua,b, ShixueDoub,n, HuakunLiub, LimingDaia,nn, Nano Energy(2013) 2, 439–442.

[6] Lipson, A. L.; Han, S.-D.; Pan, B.; See, K. A.; Gewirth, A. A.; Liao, C.; Vaughey, J. T.; Ingram, B. J., "Practical Stability Limits of Magnesium Electrolytes". Journal of The Electrochemical Society 2016, 163, (10), A2253-A2257.

[7] Bitenc J and Dominko R (2018)," Opportunities and Challenges in the Development of Cathode Materials for Rechargeable Mg Batteries". Front. Chem. 6:634. doi:10.3389/fchem.2018.00634.

[8]Zhong G, Gong J, Wang C, Xu K and Chen H (2018), "Comparison of the Electrochemical Performance and Thermal Stability for Three Kinds of Charged Cathodes." Front. Energy Res. 6:110. doi: 10.3389/fenrg.2018.00110.

[9]Haegyeom Kim et al Investigation of Potassium storage in Layered P3-Type K_0.5 MnO_2 cathode", Adv. Mater. 2017, 29, 1702480. doi: 10.1002/adma.201702480.

[10] Frayret, C.; Villesuzanne, A.; Spaldin, N.; Bousquet, E.; Chotard, J. N.; Recham, N.; Tarascon, J. M. "LiMSO4F (M = Fe, Co and Ni): promising new positive electrode materials through the DFT microscope". Phys. Chem. Chem. Phys. 2010, 12, 15512–15522

[11] Jungwoo Woo et al, "Theoretical dopant screening and processing optimization for Vanadium disulfide (VS_2) as cathode material for Li-air batteries: A DFT study", Applied Surface Science 508 (2020) 145276. doi.org/10.1016/j.apsusc.2020.145276.

[12]. Yuting Xie et al, "Deep insight into the Lithium transportation mechanism and lithium deintercalation study on Ɛ-LiVOPO_4 cathode material by atomistic simulation and first principles method", Journal of Power Sources 503 (2021) 230061, doi.org/10.1016/j.jpowsour.2021.230061.
[13]. S Kirklin et al (2015), 'The Open Quantum Materials Database (OQMD) assessing the accuracy of DFT formation energies', Computational materials Journal, issue No.1,volumeNo.15010;Doi:10.1038/npjcompumats.2015.10
[14]. Aydinol, M. K.; Kohan, A. F.; Ceder, G.; Cho, K.; Joannopoulos, J. "Ab initio study of lithium intercalation in metal oxides and metal dichalcogenides". Phys. Rev. B: Condens. Matter Mater. Phys. 1997, 56 (3), 1354−1365.
[15]. Meng, Y. S.; Arroyo-de Dompablo, M. E. "First principles computational materials design for energy storage materials in lithium-ion batteries". Energy Environ. Sci. 2009, 2 (6), 589−609.
[16]. M. Saiful Islam and Craig A. J. Fisher, "Lithium and sodium battery cathode materials: computational insights into voltage, diffusion and nanostructural properties", Chem. Soc. Rev., 2014, 43, 185.
[17]. W. Hu, H.W. Wang, W.W. Luo, B. Xu, C.Y. Ouyang, "Formation and thermodynamic stability of oxygen vacancies in typical cathode materials for Li-ion batteries: Density functional theory study," Solid State Ion. 347 (2020), 115257.
[18]. Islam, M. S.; Fisher, C. A. "Lithium and sodium battery cathode materials: computational insights into voltage, diffusion and nanostructural properties". Chem. Soc. Rev. 2014, 43 (1), 185−204.
[19]. Y.H. Chen, J. Zhang, Y. Li, Y.F. Zhang, S.P. Huang, W. Lin, W.K. Chen, "Effects of doping high-valence transition metal (V, Nb and Zr) ions on the structure and electrochemical performance of LIB cathode material LiNi0.8Co0.1Mn0.1O2," Phys. Chem. Chem. Phys. 23 (2021) 11528–11537.
[20]. W. Hu, H.W. Wang, W.W. Luo, B. Xu, C.Y. Ouyang, Formation and thermodynamic stability of oxygen vacancies in typical cathode materials for Li-ion batteries: Density functional theory study, Solid State Ion. 347 (2020), 115257.